Persistent luminescence of $ZnGa_2O_4$: Cr, an outstanding biomarker for *in vivo* imaging

S. K. Sharma [a], A. Bessiere [a], D. Gourier [a], L.Binet [a], B.Viana [a],
N. Basavaraju [b], K. R. Priolkar [b],
T. Maldiney [c], D. Scherman [c], C. Richard [c]

[a] IRCP, Institut de Recherche de Chimie Paris, CNRS- Chimie Paristech,
11 rue P&M Curie 75005 Paris, France
[b] Department of Physics, Goa University, Taleigao plateau, Goa 403206, India.
[c] Unité de Technologies Chimiques et Biologiques pour la Santé; UMR 8256 CNRS; U 1022 Inserm;
Université Paris Descartes, Sorbonne Paris Cité, Faculté des Sciences Pharmaceutiques et Biologiques,
Paris, F-75270 cedex France; Chimie-ParisTech, Paris, F-75231 cedex France.

* Author for correspondence: bruno.viana@chimie-paristech.fr

ABSTRACT

$ZnGa_2O_4$ (ZGO) is a normal spinel. When doped with Cr^{3+} ions, ZGO:Cr becomes a high brightness persistent luminescence material with an emission spectrum perfectly matching the transparency window of living tissues. It allows *in vivo* mouse imaging with a better signal to background ratio than classical fluorescent NIR probes. The most interesting characteristic of ZGO:Cr lies in the fact that its LLP can be excited with red light, well below its band gap energy and in the transparency window of living tissues. A mechanism based on the trapping of carriers localized around a special type of Cr^{3+} ions namely Cr_{N2} can explain this singularity. The antisite defects of the structure are the main responsible traps in the persistent luminescence mechanism. When located around Cr^{3+} ions, they allow, via Cr^{3+} absorption, the storage of not only UV light but also all visible light from the excitation source.

Keywords: Persistent Luminescence; Long-Lasting Phosphorescence, chromium doped $ZnGa_2O_4$; *In vivo* Optical Imaging, Mechanism.

I. INTRODUCTION

Optical imaging constantly demands more sensitive tools for biomedical research and medical applications. Long-lasting phosphorescence (LLP) nanoparticles emitting in the near-infrared (NIR) have been recently introduced to enable highly sensitive *in vivo* imaging of small animals [1]. The LLP must be located in the "biological optical window", where tissues are the most transparent, i.e. between 600 nm and 1100 nm [2]. The proof-of-concept was first reported by our groups in 2007 using $Ca_{0,2}Zn_{0,9}Mg_{0,9}Si_2O_6 : Eu^{2+}, Dy^{3+}, Mn^{2+}$ nanoparticles as the original red LLP markers. A persistent luminescence signal was detected in mouse vasculature for up to one hour after systemic injection [1]. By using persistent nanophosphors (otherwise termed as long-lasting phosphors) ultraviolet (UV) excitation of the biomarker is realized *ex vivo* before its injection to the animal avoiding tissues autofluorescence [1] This imaging technique has been improved by enhancing the persistent luminescence efficiency of various red-emitting silicates [3, 4] and phosphates [5]. Most recently a new candidate for near-infrared LLP marker has been unveiled with $ZnGa_2O_4:Cr^{3+}$ (ZGO:Cr) presenting highly enhanced LLP properties [6].
IRCP laboratory –previously named LCMCP- has now a long experience in the characterization of the luminescence properties of materials [7-13].
$ZnGa_2O_4$ crystallizes in the normal spinel structure (space group Oh^7 (Fd3m)) with Zn^{2+} ions occupying tetrahedral sites and Ga^{3+} ions occupying octahedral sites. Cr^{3+} doping ion substitutes octahedrally coordinated Ga^{3+} host cation. When excited, Cr^{3+} emits *via* its ^2E (^2G) → $^4A_2$ (^4F) d-d transition, a NIR luminescence peaking at 696 nm, a suitable wavelength for *in vivo* imaging (transmission maximum of biological tissues). Long-lasting phosphorescence originates from specific point defects of the material that trap free carriers generated during the excitation period [12]. The aim of the paper is to discuss LLP features in $ZnGa_2O_4$ and to discuss the LLP mechanism.

Optical Components and Materials XI, edited by Michel J. F. Digonnet, Shibin Jiang,
Proc. of SPIE Vol. 8982, 898215 · © 2014 SPIE · CCC code: 0277-786X/14/$18
doi: 10.1117/12.2041838

II. PRINCIPLE OF *IN VIVO* IMAGING

When emitting at appropriate wavelength, LLP materials can be used as luminescent bio-markers *in vivo*. For this, they are designed as nanoparticles able to circulate into the blood vessels of a small animal. Though intended for diagnosis applications in living animals, first generation LLP probes (silicates and phosphates) suffered from several limitations. In particular, the first generation of persistent luminescence nanoparticles had to be excited *ex vivo* by UV light prior its systemic administration, producing a persistent luminescence signal only detected until 1 hour after the injection, preventing long-term imaging in living animal. Thus, this first generation probes does not allow observing *in vivo* tumour homing strategies such as those relying on slow accumulation of stealth nanocarriers within malignant stroma by the enhanced permeability and retention effect [14,15]. Depending on the nanoparticle characteristics, such retention process usually requires from 2 to 24 hours [16,17]. This is far too long in relation to the emission from persistent luminescence nanoparticles, which hardly exceeds one hour *in vivo*.

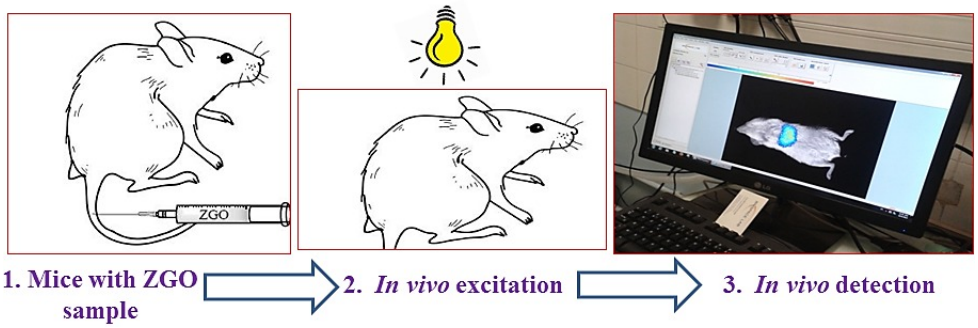

Figure 1: Various steps of in vivo optical imaging of small animal.

In a major improvement in the technique, a second generation of materials was developed [6,12]. The overall principle is to excite and detect red-emitting LLP materials for an application of *in vivo* imaging. In a typical experiment, nanoparticles dispersed in biological medium were injected to mice (Figure 1- step 1). With the second generation materials, prior *ex vivo* excitation is possible but is not necessary as was the case with first generation silicate and phosphate LLP probes. The nanoparticles thus injected are allowed to circulate into the blood vessels of small animal for some time. An *in vivo* excitation is performed when needed using orange-red light (580nm) (Figure 1- step 2). After the end of the excitation, the carriers are progressively detrapped by thermal activation to feed LLP probes and are detected using suitable imaging camera (Figure 1-step 3). With such nanoprobes (ZGO:Cr or others compounds in the spinel family), *in vivo* excitation is possible and long-term imaging could be envisioned. This constitutes a considerable progress compared to the first generation of nanoprobes.

III. MATERIAL PREPARATION AND OPTICAL CHARACTERIZATION

ZGO:Cr powder could be synthesized by solid state and hydrothermal methods [6,12]. For solid state compounds, appropriate quantities of ZnO, Ga_2O_3 and CrO_3 were mixed and carefully ground in an agate mortar with propan-2-ol. A pellet was prepared from the powder mixture and fired in air at 1300°C. The compound was prepared with a Cr content of 0.25, 0.5 and 0.75 at. % relatively to Ga. A nominal 1% Zn deficiency relative to stoichiometry was introduced in the reactants ratio as this was shown to improve LLP of ZGO : Cr powders prepared by solid state route. We infer that this small Zn deficiency provides best compensation for the parallel evaporation of ZnO and Ga_2O_3, achieving longest range order. X-ray diffraction assessed a cubic phase free from any impurity.

For thermally stimulated luminescence (TSL) measurements, the sample was prepared as a thin pressed pellet and silver glued on the cold finger of a cryostat, was excited at 10K across the cryostat quartz window. The excitation was carried out with monochromatic excitation produced by the third harmonic of a YAG:Nd pulsed laser pumped by an

OPO. TSL was detected via an optical fiber using a Scientific Pixis 100 CCD camera cooled at -65°C coupled with an Acton SpectraPro 2150i spectrometer for spectral analysis while a heating rate of 10 K/min was applied. TSL glow curves were drawn by plotting the integrated luminescence intensity over 640-760 nm. LLP measurements were carried out on 0.2 g powder samples stacked into 1 cm-diameter sample-holder. The sample was first excited for 15 min with a monochromatic excitation provided by the third harmonic of a YAG:Nd pulsed laser pumped by an Optical Parametric Oscillator (OPO). The excitation was also performed using standard 6W UV tube (with prominent emission at 254 nm) for comparison. Its luminescence was detected via an optical fiber using a Scientific Pixis 100 CCD camera cooled at -65°C coupled with an Acton SpectraPro 2150i spectrophotometer for spectral analysis.

IV. THERMOLUMINESCENCE RESULTS

The glow curves normalized to the main peak intensity are presented in Figure 2 for 290 nm and 550 nm excitation wavelength. Different excitation wavelengths were selected along the TSL excitation ranging between 230 nm and 680 nm. First a TSL glow curve was recorded with 680 nm (1.8 eV) visible light, corresponding to the low energy tail of the $^4A_2 \rightarrow {}^4T_2$ and the spin forbidden $^4A_2 \rightarrow {}^2E$ transitions. The TSL intensity is very weak but was still clearly observable (not presented).

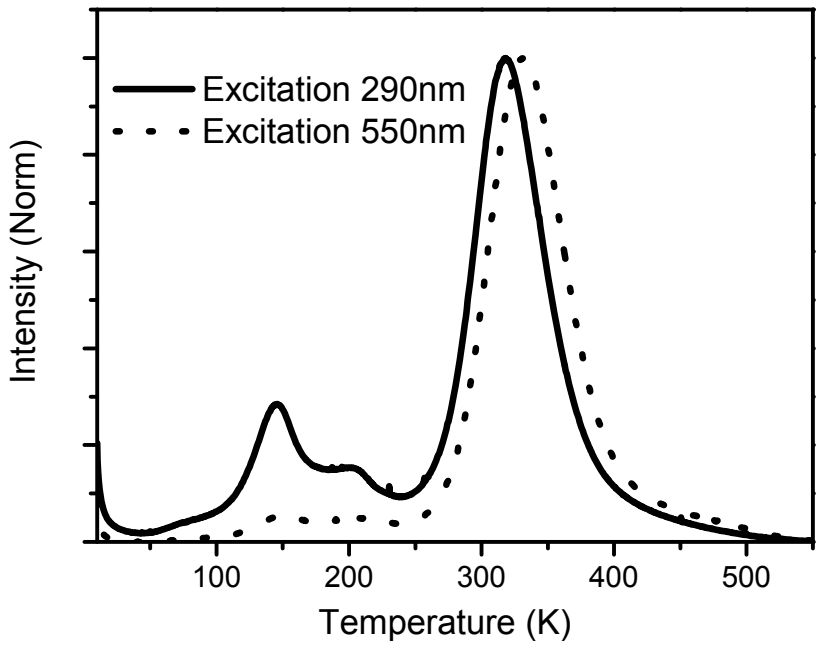

Figure 2. Normalized TSL glow curve with 290 nm and 550 nm.

As excitation wavelength shortens, the intensity of these low temperature peaks grows up relative to the main peak, with a maximum relative intensity for 230 nm (5.4 eV) excitation. Moreover, varying the excitation wavelength induces a shift in the position of the main peak maximum (see Figure 2). This gives another indication that the mechanism of charge trapping/detrapping is localized in the close vicinity of Cr^{3+} ions, as $^4T_2$ and ^2E are well below the conduction band (CB) edge [12].

Figure 3 shows on the one hand, the variation in the peak intensity at 145 K (noted I_{145}) as a function of the excitation energy (right scale) and on the other hand, the glow curve temperature maximum (noted T_{max}) as a function of the excitation energy (left scale). For excitations below 400 nm (above 3.1 eV), the peak maximum is observed around 318 K while excitations above 400 nm lead to a maximum shifted around 333 K. Applying a thermal cleaning procedure to this main peak showed that the latter was not a single peak but was made of a continuous distribution of peaks. Therefore, the shift in peak maximum observed could be explained by the presence of several traps at slightly varying trap depths, more or less involved depending on the excitation energy. Below 400 nm excitation (above 3.1 eV), the shallowest traps of the distribution are filled, which shifts the peak to lower temperature, while excitation

above 3.1 eV leads to the filling of the deepest traps and shifts the peak to higher temperature. Therefore, we observe two distinct behaviors upon increasing the excitation wavelength. The low temperature TSL peaks on the one hand shows an intensity that decreases with lower excitation energy, while the main broad TSL peak on the other hand exhibits a shift of the temperature maximum towards high temperature. These two behaviors show a monotonous trend but also an abrupt change across the border value of ≈3.1 eV. This indicates again a change of regime in the TSL process at the photon energy threshold of 3.1 eV [12].

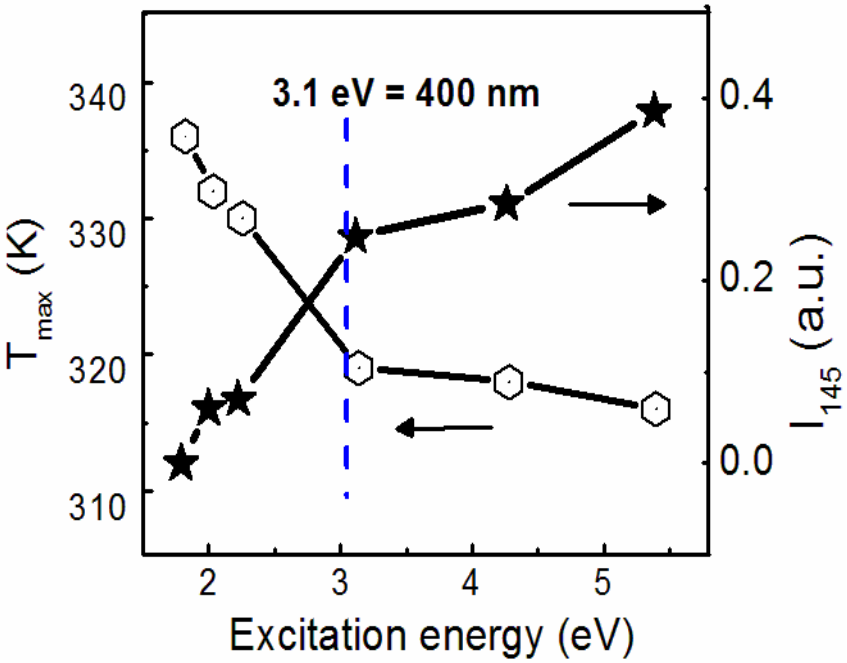

Figure 3. Variation of TSL glow curve maximum and TSL intensity for 145K glow curve maximum.

The above results indicate that the LLP mechanism is localized around Cr^{3+} ions for low photon energy excitation (down to 680 nm), corresponding mainly to the $^4A_2 \rightarrow {}^4T_2$ transition. We may then consider that shorter wavelength (higher energy) excitation allows a charge separation over longer distance and/or at longer distances from Cr^{3+} centers. The farthest traps being the shallowest, the TSL peak tends to shift to lower temperature when shorter excitation wavelength is used. The shallow traps corresponding to low temperature TSL peaks (145 K and 200 K) present a different behavior. They are easily filled with excitation above 3.1 eV but very less efficiently filled for excitation below 3.1 eV. Further, those peaks show as intense Cr_R emission as Cr_{N2}, which means that all Cr^{3+} ions are involved in this case [12]. As these shallow traps are filled through band-assisted excitation, they may be located below the bottom of the CB and above the top of the VB, and at long distances from Cr^{3+} ions.

V. LLP DECAY AND LLP MECHANISM

The LLP decay in ZGO:Cr^{3+} is shown in Figure 4 for 290 nm and 550 nm excitation wavelength. Persistent luminescence in ZGO:Cr is of high interest for *in vivo* optical imaging. Excitation of ZGO:Cr in the form of nanoparticles with UV light *before* their injection to a small animal is possible and triggers a LLP signal observable across the animal tissues for a couple of hours (similarly to the LLP decay after 290 nm excitation shown in Figure 4). Furthermore, a subsequent excitation with red light across the animal tissues *after* their injection enables the excitation of the LLP decay (similarly to the LLP decay after 550 nm excitation shown in 4). The LLP of the probes inside the animal can therefore be excited many times over a very long period (several days). This is an essential property of the material that enables to follow *in vivo* the slow accumulation of LLP nanoparticles in tumors [18]. Experimental results on ZGO:Cr also showed that LLP induced by direct excitation of Cr^{3+} involves no change of its valence state [12], i.e. the metal ion does not liberate an electron (leading to Cr^{4+}) or a hole (leading to Cr^{2+}).

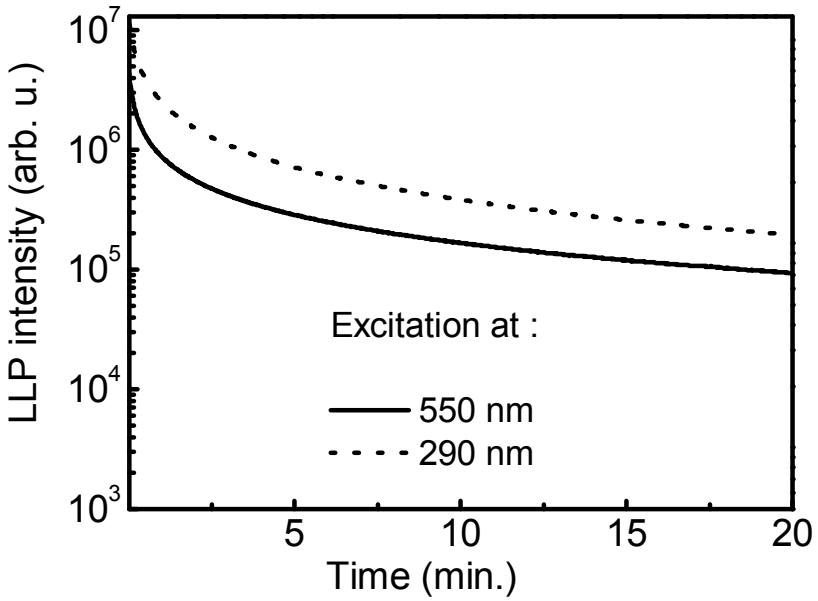

Figure 4. LLP decay curves at 290 nm and 550 nm excitation wavelength.

Moreover the fact that LLP can be excited by orange-red light questions the usually compulsory participation of host bands to LLP. The present work shows several indications that the LLP mechanism in ZGO:Cr involves release and trapping of neutral electron-hole pairs and that this mechanism is localized in the vicinity of Cr_{N2} ions. The detailed LLP mechanism is illustrated in Figure 5.

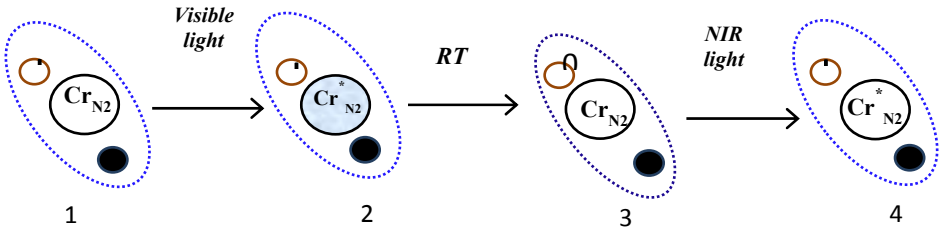

Figure 5. LLP in ZGO:Cr induced by excitation below 3.1 eV. Cr_{N2} is represented by its states ($^4T_2$, $^4A_2$ or ^2E). Steps: 1) optical excitation; 2) charge separation and carriers trapping by neighboring antisite defects of opposite charges; 3): thermal release of e^--h^+ pairs and trapping by Cr^{3+}; 4): emission. Filled and empty spheres represent the two opposite charge antisite defects.

We propose in the following a mechanism based on the existence of a cationic disorder in spinels. The first step is the excitation of Cr_{N2}, for instance in the $^4T_2$ state by optical illumination at 550 nm (step 1 in Figure 5). The excitation, initially localized at Cr_{N2}, is then dissociated by the local electric field into an electron and a hole that get trapped at Ga°_{Zn} and $Zn^{'}_{Ga}$ neighboring defects, respectively (step 2 in Figure 5). The excitation is trapped in the vicinity of chromium in the form of a pair of neutral defects Ga^{x}_{Zn} and Zn^{x}_{Ga} while Cr^{3+} returns to its $^4A_2$ ground state (step 2 in figure 5). The electron (or hole) trapping by Ga_{Zn} (Zn_{Ga}) is thus strictly equivalent to an optically induced donor-acceptor (D-A) transfer from Zn_{Ga} (D) to Ga_{Zn} (A). It is important to note that the local electric field responsible for charge separation in the excited state of Cr_{N2} vanishes as the antisite defects become neutral after electron-hole trapping. The reverse reaction (electron-hole release and capture by Cr^{3+}) is thermally activated; with the activation energy E_{dt} (deep trap) responsible for the main TSL peak around 318K, in accordance with steps 3 and 4 in figure 5.

VI. CONCLUSIONS

In the present paper we investigated the mechanism of this LLP, activated by virtually all wavelengths of the UV and visible range. We took advantage of Cr^{3+} that constitutes by substituting Ga^{3+} in the spinel structure, a very fine optical and paramagnetic probe of its local environment. We could therefore demonstrate that LLP occurred via the excitation of a specific type of Cr^{3+} ions, namely Cr_{N2}, having an antisite defect as first cationic neighbor. Exciting ZGO:Cr in any of the absorption bands of Cr_{N2} all over the visible range (down to 680 nm) therefore triggers LLP. An efficiency amplification by band assistance is however clearly shown to exist above the threshold value of 3.1 eV (400 nm) due to the position of Cr^{3+} states relative to free e^--h^+ states. LLP can therefore take place at low photon energy without any participation of the host bands following a mechanism entirely localized around Cr_{N2}. Various different materials in the spinel family are investigated to develop news tools for *in vivo* imaging [18-20].

ACKNOWLEDGMENTS

Authors acknowledge the Indo-French Centre for the Promotion of Advanced Research (IFCPAR)/ CEntre Franco-Indien Pour la Recherche Avancée (CEFIPRA) for financial support.

REFERENCES

[1] le Masne de Chermont, Q., Chanéac, C., Seguin, J., Pellé, F., Maîtrejean, S., Jolivet, J.P., Gourier, D., Bessodes, M. & Scherman, D., *Proc. Natl. Acad. Sci. USA* 104, 9266-9271 **(2007)**.
[2] Castano, A.P., Demidova, T.N., Hamblin M.R., *Photodiagnosis and Photodynamic Therapy* 1, 279—293 **(2004)**.
[3] Maldiney, T., Lecointre A., Viana, B., Bessière A., Bessodes, M., Gourier, D., Richard, C., Scherman, D., *J. Am. Chem. Soc.* 133, 11810-11815 **(2011)**.
[4] T. Maldiney, G. Sraiki, B. Viana, D. Gourier, C. Richard, D. Scherman, M. Bessodes, K. Van den Eeckhout, D. Poelman, P. F. Smet. *Opt. Mat. Express* 2, 261-268 **(2012)**.
[5] Bessiere, A., Lecointre, A., Ait Benhamou, R., Suard, E., Wallez, G., Viana, B. *J. Mater. Chem. C*, *1*, 1252 **(2013)**.
[6] Bessière A., Jacquart, S., Priolkar, K., Lecointre, A., Viana, B. & Gourier, D., *Opt. Express* **19,** 10131-10137 **(2011)**.
[7] Lecointre A., Bessière A., Bos, A.J.J., Dorenbos, P., Viana, B., Jacquart, S. *J. Phys. Chem. C,* 115, 4217–4227 **(2011)**.
[8] Bos, A.J.J., Dorenbos, P., Bessiere, A., Viana, B., *Radiation Measurements* 43 2-6 222-226 **(2008)**.
[9] Koslova, N., Viana, B., Sanchez, C., *Journal of Materials Chemistry* 3 1 111-112 **(1993)**.
[10] Cordoncillo, E.; Guaita, F.J., Escribano, P., *Optical Materials* 18 3 309-320 **(2001)**.
[11] Maldiney, T., Viana, B., Bessiere, A.,Gourier, D., Bessodes, M., Scherman, D., Richard, C., *Optical Materials* 35 10 1852-1858 **(2013)**.
[12] Bessiere, A, Sharma, S.K., Basavaraju, N., Priolkar, K.R., Binet, L., Viana, B., Bos, A.J.J., Maldiney, T., Richard, C., Scherman, D., Gourier., D., *Chem. Mater.*, DOI: 10.1021/cm403050q *in Press* **(2014)**.
[13] Basavaraju, N., Sharma, S., Bessiere, A., Viana, B., Gourier, D., Priolkar, K.R., *J. Phys. D : Appl. Phys*. 46, 375401 **(2013)**.
[14] Jain, R.K. & Stylianopoulos, T. *Nat. Rev. Clin. Oncol.* **7,** 653-664 **(2010)**.
[15] Danhier, F., Feron, O. & Préat, V. *J. Control. Release* 148, 135-146 **(2010)**.
[16] Al-Jamal, W.T., Al-Jamal, K.T., Tian, B., Cakebread, A., Halket, J.M. & Kostarelos, K. *Mol. Pharm.* 6, 520-530 **(2009)**.
[17] Park, J.H., Gu, L., von Maltzahn, G., Ruoslahti, E., Bhatia, S.N., Sailor, M.J. *Nat. Mater.* 8, 1-6 **(2009)**.
[18] Maldiney, T., Bessière, A., Seguin, J., Teston, E., K. Sharma, S.K. Viana, B., Bos, A.J.J., Dorenbos, P., Bessodes, M; Gourier, D.,Scherman, D., Richard, C. *Nat Mater. In Press* **(2014)**.
[19] Pan, Z., Lu, Y.Y., Liu, F. *Nat. Mater.* 11, 58-63 **(2012)**.
[20] Zhuang, Y.X., Ueda, J., Tanabe, S., *Applied Physics Express* 6 5 052602 **(2013)**.